Evaluation of Stability of Silicon-Photonics-Based Optical Switch Network Architectures against Parasitic Errors in Switch Elements

Banafsheh Abasahl , Wim Bogaerts

Ghent University - Imec, Technologiepark 126, 9052 Ghent, Belgium
Center of Nano-and Biophotonics, Ghent University, Ghent, Belgium e-mail: banafsheh.abasahl@imec.be

ABSTRACT

The performance of MEMS-based optical switch networks against losses and parasitic effects in tunable elements for different architectures are simulated. A comparison between those architectures is provided considering the fact that the parasitic effects of MEMS switches are highly depend on their status.

Keywords: optical switch networks, MEMS switches, Beneš, PILOSS, cross-bar, optical circuit simulation, stochastic analysis, errors.

1 INTRODUCTION

Optical switch networks are essential platforms for all-optical communication networks. The power consumption and cost of communication networks drop dramatically if low-power and high performance silicon photonic integrated circuits with tunable components are incorporated in such networks. In order to maintain the performance of these networks in larger scales, the choice of switch architecture (i.e. the connectivity network inside the switch) is crucial. The performance of these switch networks not only depend on components losses, but also on parasitic coupling effects. These effects can give rise to distortion in the output signals, non-uniformity and crosstalk due to multi-path interference. In this work, we provide a comparison between different architectures that can be implemented in a photonic integrated circuit (PIC). Three non-blocking architectures for N×N switch networks, namely cross-bar, path-independent loss (PILOSS) [1] and Beneš [2] are implemented. A schematic representation of these networks is shown in Fig. 1. We consider a silicon photonics technology platform, but as switching elements we introduce the use of of optical MEMS [3], [4], because these switches, as opposed to optical switches based on electric heating [5], offer almost zero electric power loss at the expense of low switching speed.

2 IMPLEMENTATION OF SWITCH NETWORK ARCHITECTURES

The switch elements in this work are based on MEMS directional couplers (DC) where the spacing between the waveguides can be mechanically adjusted. For these tunable DCs, in the *bar* state, the two waveguides are
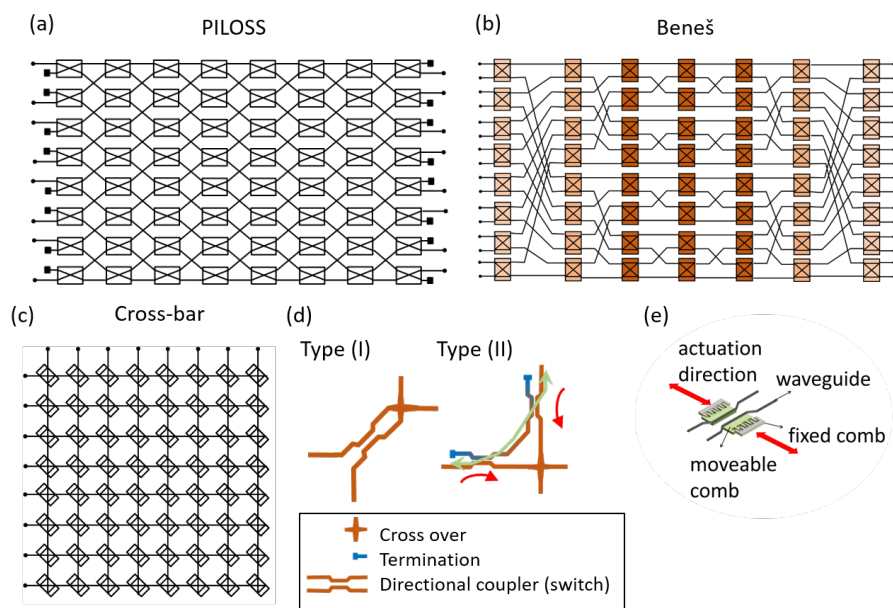

Figure 1. Switch network architectures under consideration: (a) Beneš, (b) PILOSS, and (c) Cross-bar. (d) two types of switch implementations for the cross-bar architecture, (e) a schematic representation of a MEMS directional coupler with comb actuation. Although the calculations are performed on 16×16 networks, here for the sake of clarity, 8×8 networks are presented for cross-bar and PILOSS architectures.
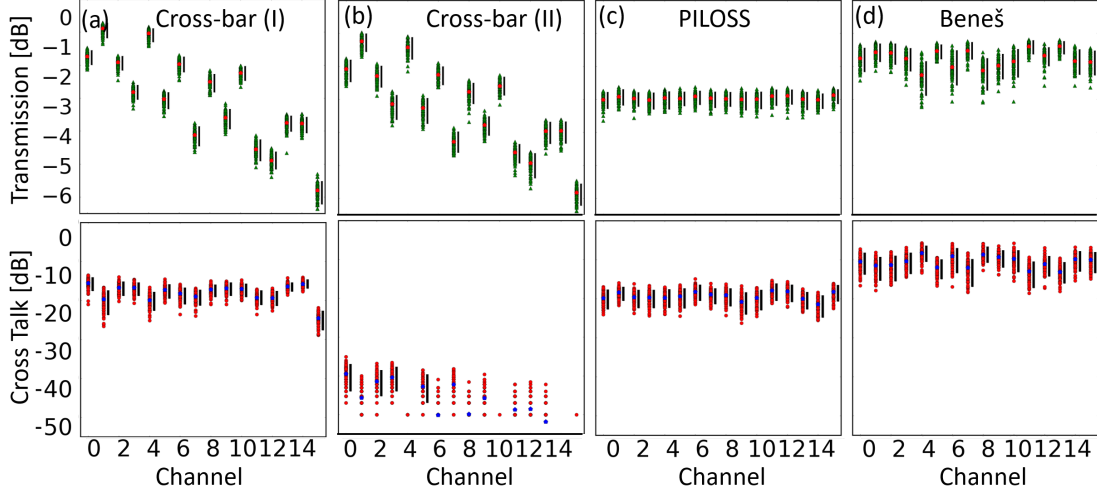
Figure 2. Distribution of the transmission (top) and cross talk (bottom) of 100-cycle Monte Carlo simulations with $\sigma_{cross} = 5\%$ for 16×16 networks with (a) cross-bar(I), (b) cross-bar (II), (c) PILOSS and (d) Beneš architectures.

sufficiently far apart that no coupling occurs. On the other hand, the two waveguides are brought close together in the *cross* state and the DC becomes more sensitive to the coupling distance and therefore it introduces higher error levels and wavelength dependence in the coupling.

The cross-bar architecture comprises of a matrix of N×N switches. The switches are always in the bar state except for the switches SE_{mn}, where the input m^{th} is to be routed to the output n^{th}. In contrast to the cross-bar architecture where the number of switches (N_{switch}) and crossovers ($N_{crossover}$) depend on the requested mapping, the PILOSS architecture offers a solution where these numbers are always constant. In each routing, only one switch is in the *bar* state, and the the rest are in *cross* states, which is not conducive for low losses and errors. In order to benefit from the performance of the DCs in the *bar* state, a combination of a DC and a cross over, like the switch shown for cross-bar type(I), is used. In this case, the 100% transmission correspond to *cross* state. For each of these two architectures N^2 switches are needed, which results in a large footprint and an accumulation of errors and losses.

A more compact solution is a routine proposed by Beneš where $N = 2^p$ inputs-outputs are routed in a layered architecture. In this case, the number of switches per routing decreases dramatically. The physical properties of the three architectures as a function of the number of input-outputs (N) are provided in Table 1. The simulations are performed for $N = 16$ using the Caphe circuit simulator by Luceda Photonics, extended with our own variability analysis routines [6]. In order to study the effect of stochastic imperfections of switches, in a 100-loop Monte-Carlo set of simulations, the coupling values assigned to each DC is randomly deviated from its ideal setting of 0 (*bar*) or 1 (*cross*), with a normal probability distribution and a standard deviation of σ_{bar} and σ_{cross}. In each case, the σ_{cross} is considered to be one order of magnitude larger than σ_{bar}. The insertion loss for the *bar* and *cross* states are considered to be 0.3 dB and 0.4 dB, respectively. For the cross-bar architecture, the performance is evaluated by incorporating two types of switch nodes, shown Fig. 1a: type (I) with a single DC and a crossover, as those considered for the other two architectures, and type (II) built of two DCs and one crossover suggested in [4]. The resulting distribution for the outputs of 16×16 networks with the these architectures are shown in Fig. 2a-d for a $\sigma_{cross} = 5\%$ and $\sigma_{bar} = 0.5\%$. The simulator evaluates the S-parameter between each input-output pair, from which the transmission and the crosstalk values are inferred. In Table 1, the outcomes of Monte-Carlo simulations, averaged over the 100 cycles and the 16 outputs, are presented.

TABLE 1. COMPARISON BETWEEN PROPERTIES OF THE THREE SWITCH NETWORK ARCHITECTURES. THE VALUES IN RED ARE FOR A 16×16 NETWORK. THE AVERAGE VALUES CALCULATED FOR $\sigma cross = 5\%$ AND $\sigma_{bar} = 0.5\%$ ARE PRESENTED IN BLUE.

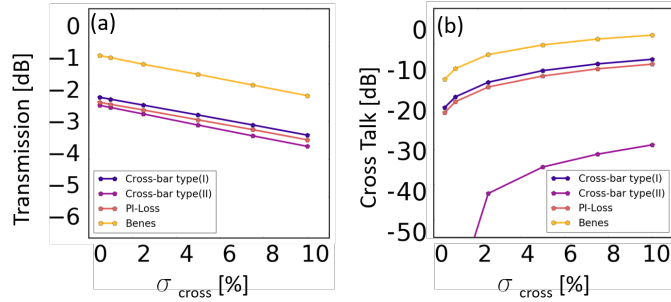|	Cross bar (I)	Cross bar (II)	PILOSS	Beneš
N_{DC} ; $N_{crossover}$	$N^2;N^2$	$2N^2;N^2$	$N^2;N^2 + (N-1)^2$	$(2 \times \log_2 N - 1) \times \frac{N}{2}; \sum_{m=0}^{\log_2 N} (\frac{N^2}{2^m} - N)$
	256; 256	512; 256	256; 225	56; 88
N_{switch} per path	1 to $2N-1$	1 to $2N-1$	N	$2\log_2 N - 1$
	1 to 33	1 to 33	16	7
N_{rs}	4	4	4	-
	4	4	4	1 to 29 (Average= 10)
Transmission	-2.83 dB	-3.11 dB	-2.96 dB	-1.75 dB
Crosstalk	-17.68 dB	-45.04 dB	-19.22 dB	-10.38 dB

Figure 3. Average transmission (a) and cross talk (b) of the 16 channels as a function of σ_{cross}, when $\sigma_{bar} = 0.1\sigma_{cross}$ for the four architectures of Fig. 1.

3 DISCUSSION

Among the the mentioned architectures, the Beneš network with the smallest $N_{switche}$ and $N_{crossover}$ offers the minimum footprint, the lowest insertion loss and therefore the highest transmission, as can be seen in Fig. 3a. On the other hand, based on Fig. 3b, it suffers from the highest crosstalk due to the number of switches in the *cross* state being dependent on the requested map. In addition, Beneš network is indeed rearrangably non-blocking, i.e. when two sets of input-output are altered, at least one more switch must be altered. This causes a cutoff period in the other outputs which are still mapped to the same inputs. Our calculations show that for a 16×16 Beneš architecture depending on the rearrangement, N_{rs}=1 to 29 switches (with an average of 10) are needed to alter for an alteration of two input-output sets. For cross-bar and PILOSS architectures, N_{rs}=4 and the outputs experience no cutoff unless they are altered.

The number of switches and crossovers for the path between each input-output pairs is constant for Beneš and PILOSS configurations, regardless of the requested mapping. For the PILOSS configuration, as can be inferred from 2c, since there is always only one switch in the *cross* state per path, the signal and cross talk levels show the most independence to the requested mapping. On the other hand, for the cross-bar architectures, the number of elements in each path differs for each input-output combination and it can range from one switch and one crossover (when the last input is mapped to the first output) to $2N - 1$ switches and crossovers (when the first input is mapped to the last output). In Fig. 2a and b, the average transmission level varies from, respectively, -0.8 dB and -1.2 dB in the second channel to, respectively, -5.7 dB and -5.8 dB in the last channel. For the Beneš network in Fig. 2d, transmission varies from -1.34 dB to -2.22 dB, while this variation reduces to 0.15 dB for the PILOSS architecture in Fig.2c. Among the studied architectures in this work, cross bar type (II) presents the lowest cross talk, due to its switch design. In fact, the errors in the DCs are bypassed to terminals and are prevented to propagate in the network. The terminals are considered to be connected to light sinks with a negligible back-reflection.

ACKNOWLEDGEMENT

REFERENCES

[1] K. Suzuki, K. Tanizawa, T. Matsukawa, G. Cong, S.-H. Kim, S. Suda, M. Ohno, T. Chiba, H. Tadokoro, M. Yanagihara, Y. Igarashi, M. Masahara, S. Namiki, and H. Kawashima, "Ultra-compact 8 8 strictly-non-blocking Si-wire PILOSS switch," Optics Express **22**, 3887–3894 (2014).

[2] H. NAKAJIMA, "Development on Guided-Wave Switch Arrays," IEICE Trans. Electronics E **82**, 297–304 (1999).

[3] U. Shah, M. Sterner, and J. Oberhammer, "High-Directivity MEMS-Tunable Directional Couplers for 10–18-GHz Broadband Applications," IEEE Transactions on Microwave Theory and Techniques **61**, 3236–3246 (2013).

[4] N. Quack, T. J. Seok, S. Han, R. S. Muller, and M. C. Wu, "Scalable Row/Column Addressing of Silicon Photonic MEMS Switches," IEEE Photonics Technology Letters **28**, 561–564 (2016).

[5] Y. Sun, Y. Cao, Y. Yi, L. Tian, Y. Zheng, J. Zheng, F. Wang, and D. Zhang, "A low-power consumption MZI thermal optical switch with a graphene-assisted heating layer and air trench," RSC Advances **7**, 39922–39927 (2017).

[6] W. Bogaerts, U. Khan, and Y. Xing, "Layout-Aware Yield Prediction of Photonic Circuits," IEEE International Conference on Group IV Photonics pp. 93–94 (2018).